RELIABILITY BASED TOPOLOGY OPTIMIZATION OF STRUCTURES UNDER STRESS CONSTRAINTS

R.B. SANTOS, A.J. TORII, AND A.A. NOVOTNY

Abstract. In this paper we propose an approach for Reliability Based Design Optimization where a structure of minimum weight subject to reliability constraints on the effective stresses is sought. The Reliability Based Topology Optimization (RBTO) problem is formulated by using the Performance Measure Approach and the Sequential Optimization and Reliability Assessment method is employed. This strategy allows for decoupling the RBTO problem into two steps, namely, a deterministic topology optimization and a reliability analysis. In particular, the deterministic structural optimization problem subject to stress constraints is addressed with an efficient methodology based on the topological derivative concept together with a level-set domain representation method. The resulting algorithm is applied to some benchmark problems, showing the effectiveness of the proposed approach.

1. Introduction

Topology optimization of continuum structures with stress constraints has been subject of intense research over the last decades [11, 25, 6, 12]. In this context, one seeks the optimum distribution of material inside a given domain that results in a structure with minimum weight and that respects constraints based on the effective stresses. Results obtained with topology optimization have a valuable field of application in the design of structures and mechanical components. In addition, in most traditional approaches, loads and material properties are considered as deterministic parameters. However, it is well known that in realistic engineering problems many parameters are subject to uncertainties. Besides, it has been observed that uncertainties consideration may lead to solutions conceptually different from deterministic optimization. This fact supports the application of optimization under uncertainties in several cases of practical interest.

Over the years, different approaches to incorporate uncertainties in the design optimization process have been proposed, see for example the reviews presented in [8, 26, 19] and references therein for details. Optimization of continuum structures considering uncertainties has been widely discussed in the literature. In particular, most works on the subject can be grouped into the classes: Robust Design Optimization and Reliability Based Design Optimization (RBDO). In the case of Robust Design Optimization, the goal is to obtain an optimum design that is least sensitive to uncertainties in the problems parameters [18, 10, 5, 29]. In the case of Reliability Based Design Optimization the constraints of the optimization problem are stated as to impose a target reliability level for the system under design [30, 22, 20].

More recently, RBDO approaches have been applied to topology optimization, originating the field of Reliability-Based Topology Optimization (RBTO) [16, 28, 13]. The main goal in RBTO is to find optimal topologies taking into account uncertainties in some parameters, such as load magnitudes and material properties. The optimum topologies obtained with RBTO are frequently different than the ones obtained with deterministic optimization alone. Recent works concerning RBTO applied to the volume minimization of structures with stress constraints were presented by [20, 27], while design of Microelectromechanical systems has been presented in [22, 17].

The goal of this paper is to present an approach based on the topological derivative concept for Reliability Based Topology Optimization (RBTO), where a structure of minimum weight subject to von Mises stress constraints under load and material uncertainties is sought. Following

Key words and phrases. topology design; structural optimization; uncertainties; topological derivatives.

the original ideas presented in [29] in the context of compliance minimization under uncertainties, the RBTO problem is formulated using the Performance Measure Approach (PMA) [30] and the Sequential Optimization and Reliability Assessment (SORA) approach [9] is employed. This strategy allows for decoupling the RBTO problem into two steps, namely, a deterministic topology optimization step and a reliability analysis step. The deterministic structural topology optimization problem subject to stress constraints is addressed with an efficient algorithm based on the topological derivative of the associated objective functional combined with a level-set representation of the structure domain [4].

There are two main advantages in using the topological derivative concept in the context of topology optimization under uncertainties, which are: (i) from the mathematical point of view, this concept has been proved to be robust with respect to uncertain data [15] and, (ii) it provides an analytical (exact) form for the topological sensitivity [24] which allows to obtain the optimal design in few iterations. In fact, the resulting approach leads to a topology design algorithm of remarkably efficiency and of simple computational implementation, which features only a minimal number of user-defined algorithmic parameters. In this paper therefore, the theory developed in [15] is also confirmed from the numerical point of view. At the end of this paper some benchmark problems are solved in order to show the effectiveness of the proposed approach. The numerical experiments agree well with the results that should be expected by other methods. Therefore, our approach can be seen as an alternative method for optimum design of structures with stress constraints under uncertainties.

This paper is organized as follows. We first present a brief review of RBDO with key aspects relevant to this work. The proposed approach is stated in Section 3. In particular, we describe how the SORA concept can be used to decouple the nested reliability optimization problem into a deterministic optimization step and a reliability analysis step. The resulting deterministic structural topology optimization problem is presented in Section 4, which is solved by using the topological derivative concept together with a level-set domain representation method. Some numerical examples are presented in Section 5, showing the effectiveness of the proposed approach as well as the importance of considering uncertainties in the topology optimization problem. Finally, some concluding remarks are presented in Section 6.

2. Brief review of RBDO

Historically, uncertainties in design of structures were taken into account by using safety factors. However, it is well known that the safety factor approach can be limited in a wide variety of cases, resulting in too conservative or unsafe designs. For these reasons, methods for evaluating the reliability of structures have been developed over the years [21, 23]. When constraints considering reliability measures are imposed on design optimization the resulting problem is called RBDO.

There are many different ways to formulate and solve RBDO problems [8, 26]. However, concepts related to First/Second Order Reliability Methods (FORM/SORM) are frequently employed [19]. It is well known that results obtained with FORM/SORM are only approximate in the presence of non-linear problems and random variables with non Gaussian distribution [21, 23]. Nevertheless, FORM based approaches are widely employed since the resulting numerical schemes are, in general, computationally efficient in comparison to other approaches, such as sampling based approaches. A given RBDO problem can be stated as

$$\begin{cases} \text{Minimize } f(\mathbf{d}) \\ \text{subject to: } P_{fi}(\mathbf{d},\mathbf{x}) \leq P_t, i = 1,2,...,m, \end{cases}, \tag{2.1}$$

where $\mathbf{d}$ is the design vector, $\mathbf{x}$ is a vector of random variables, P_t is the allowable probability of failure and P_{fi} is the probability of failure given by

$$P_{fi}(\mathbf{d},\mathbf{x}) = P(g_i(\mathbf{d},\mathbf{x}) > 0), \tag{2.2}$$

where g_i are limit state functions such that $g_i > 0$ indicates failure of the systems under analysis and P indicates the probability of occurrence of a given event. In the above problem we neglected deterministic constraints without loss of generality. Besides, in order to keep the notation in

accordance with the rest of this work, we have modified the standard notation encountered in literature where $g_i < 0$ indicates failure.

In the case of highly reliable systems the probability of failure results in very small values. In order to avoid numerical issues related to working with small values, the RBDO problem is generally rewritten in terms of reliability indexes. The reliability index according to the limit state g_i can be defined as

$$\beta_i(\mathbf{d}, \mathbf{x}) = \Phi^{-1}\left(1 - P_{fi}(\mathbf{d}, \mathbf{x})\right), \tag{2.3}$$

where Φ^{-1} is the inverse cumulated distribution function of the normal distribution with zero mean and unitary standard deviation. This reliability index can be evaluated exactly if the probability of failure is known or using some approximate scheme. In the case of FORM, the exact reliability index is approximated by the Hasofer-Lind reliability index, defined as the solution of the reliability analysis problem

$$\begin{cases} \beta_i^{\mathrm{HL}}(\mathbf{d}, \mathbf{x}) = \min \|\mathbf{v}\| \\ \text{subject to: } g_i(\mathbf{d}, \mathbf{x}) = 0 \end{cases} \tag{2.4}$$

with

$$\mathbf{v} = T(\mathbf{d}, \mathbf{x}), \tag{2.5}$$

where T is a transformation from $\mathbf{x}$ to an equivalent normal random vector $\mathbf{v}$ [21, 23]. Note that the reliability analysis problem searches for the realization of the random vector that is closest to the expected value $\mathbf{v} = \mathbf{0}$ and lies over the edge of the limit state $g_i = 0$. For this reason, the solution of this problem is frequently called the most probable point of failure. It is important to highlight that the Hasofer-Lind reliability index is exact only when g_i is a linear function of $\mathbf{x}$ and the random variables have Gaussian distribution [21, 23].

In this context, the RBDO problem can be rewritten in terms of reliability indexes as

$$\begin{cases} \text{Minimize } f(\mathbf{d}) \\ \text{subject to: } \beta_i(\mathbf{d}, \mathbf{x}) \geq \beta_t, i = 1, 2, ..., m, \end{cases} \tag{2.6}$$

where β_t is the target reliability index given by

$$\beta_t = \Phi^{-1}(1 - P_t). \tag{2.7}$$

In most situations the reliability index is approximated by the Hasofer-Lind reliability index, in order to reduce the computational effort required. In these cases the solution of the RBDO problem must be viewed as an approximate solution.

In the reliability index approach the above RBDO problem is solved directly using some optimization algorithm. However, it has been observed that this approach is ill conditioned, since evaluation of the Hasofer-Lind reliability index is sometimes numerically unstable. As proposed by Tu et al. [30], this issue can be avoided if the problem is reformualted adopting the PMA. In this case, the RBDO problem is rewritten as

$$\begin{cases} \text{Minimize } f(\mathbf{d}) \\ \text{subject to: } g_i(\mathbf{d}, \mathbf{x}_i^*) \leq 0, i = 1, 2, ..., m, \end{cases} \tag{2.8}$$

where $\mathbf{x}_i^*$ is solution to the inverse reliability analysis problem

$$\begin{cases} \mathbf{x}_i^* = \arg\max g_i(\mathbf{d}, \mathbf{x}) \\ \text{subject to: } \|T(\mathbf{d}, \mathbf{x})\| = \beta_t. \end{cases} \tag{2.9}$$

In the inverse reliability analysis problem we search for the realization of the random vector that most violates the limit state within a given range from the expected value, defined according to the target reliability index. This realization can be viewed as a worst case scenario, that is then considered in the constraint of the RBDO problem. It has been demonstrated that this problem is equivalent to the reliability index approach [30]. Besides, the problem is better conditioned and in general leads to more stable algorithms and better convergence rates. For this reason, the PMA, together with latter modifications, has become one of the most widespread approaches in the context of RBDO.

3. Proposed Approach

In this work we want to find the optimal design of a structure into two spatial dimensions subject to von Mises stress constraints and uncertainties on the data. Thus, we first present the corresponding deterministic optimization problem in which we are dealing with. Then, we introduce the reliability based design optimization problem. Finally, we present a strategy which allows for decoupling both problems.

3.1. **Deterministic Optimization Problem.** Let us consider an open and bounded domain $\mathcal{D} \subset \mathbb{R}^2$ with Lipschitz boundary Γ and a sub-domain $\Omega \subset \mathcal{D}$. Given a hold-all domain $\mathcal{D}$ and a stress constraint-enforcement sub-domain $\Omega^\star$, the deterministic optimization problem consists in minimizing the weight of the structure under point-wise stress constraints. Therefore, we want to find a sub-domain $\Omega^d \subset \mathcal{D}$ that solves the following constrained topology optimization problem:

$$\begin{cases} \underset{\Omega \subset \mathcal{D}}{\text{Minimize}} \ |\Omega|, \\ \text{subject to: } g_\Omega \leq 0, \ \text{a.e. } \Omega^\star \subset \Omega, \end{cases} \tag{3.1}$$

where $\Omega = \Omega^\star \cup \omega \subset \mathcal{D}$, with ω used to denote a part of Ω where the stress constraints are not enforced. Some terms in the above equations still require explanations. The quantity $|\Omega|$ represents the Lebesgue's measure of Ω (required volume of material). In addition, the constraint g_Ω is defined as

$$g_\Omega = \sigma_M - \overline{\sigma}, \tag{3.2}$$

where $\overline{\sigma}$ is the stress limit (yielding stress) and σ_M is the von Mises stress given by

$$\sigma_M = \sqrt{\frac{1}{2}\mathbb{B}\sigma_\Omega \cdot \sigma_\Omega}, \tag{3.3}$$

with $\mathbb{B} = 3\mathbb{I} - \mathrm{I} \otimes \mathrm{I}$ and I and $\mathbb{I}$ the fourth and second order identity tensors, respectively. In addition, σ_Ω represents the stress tensor.

3.2. **Reliability Based Design Optimization Problem.** As occurs in most cases of practical interest, the parameters of the structural optimization problems such as load intensities and material properties are not deterministic variables. Let $\mathbf{x} = [\mathrm{x}_i], i > 0$, be a vector of random variables that affect the stress constraint. Then, we note that the constraint g_Ω becomes a random variable itself and write $g_\Omega := g_\Omega(\mathbf{x})$. In this case the deterministic problem (3.1) can result in inefficient designs in practice. It is then necessary to ensure that designs present a sufficient reliability level.

In this work we formulate the RBDO problem using the PMA [30], so the RBTO problem can be stated as: Find $\Omega^p \subset \mathcal{D}$, such that

$$\begin{cases} \underset{\Omega \subset \mathcal{D}}{\text{Minimize}} \ |\Omega|, \\ \text{subject to: } g_\Omega(\mathbf{x}^*) \leq 0, \ \text{a.e. } \Omega^\star \subset \Omega, \end{cases} \tag{3.4}$$

where $\mathbf{x}^*$ is solution of following inverse reliability analysis problem: Find $\mathbf{x}^* \in \mathbb{R}^m$, such that

$$\begin{cases} \text{Maximize } g_\Omega(\mathbf{x}), \\ \text{subject to: } \|T(\mathbf{x})\| = \beta_t, \ \text{a.e. } \Omega^\star \subset \Omega. \end{cases} \tag{3.5}$$

where β_t is target reliability index and $\mathbf{v}$ is the normalized random vector. In the case of independent Gaussian random variables, the transformation $T : \mathbf{x} \to \mathbf{v}$ is given by

$$\mathrm{v}_i = \frac{\mathrm{x}_i - \overline{\mathrm{x}}_i}{s_i}, \tag{3.6}$$

where $\overline{\mathrm{x}}_i$ and s_i are the mean and the standard deviation of the random variables x_i. In the case where the variables have non Gaussian distributions, its is possible to apply (3.6) with equivalent mean and standard deviation obtained with some criterion, such as the normal tail approximation [14].

The solution of problem (3.5) is the point that maximizes the limit state function g_Ω within a distance equal to the minimum allowable reliability index β_t. Consequently, it can be viewed

as the Worst Case Scenario among all points distant β_t from the origin of the normalized probabilistic space. By imposing $g_\Omega(\mathbf{x}^*) \leq 0$ in problem (3.4), we are actually ensuring that the worst case scenario will not violate the original constraint of the problem.

3.3. **Decoupling Strategy.** From (3.4), we note that it is necessary to solve an optimization problem (the inverse reliability analysis problem) in order to evaluate the constraint. We thus have two nested optimization problems. Solving the nested optimization problem directly can lead to very demanding computational routines and convergence difficulties, and is not an efficient approach in most cases. For this reason, several FORM based decoupling approaches have been proposed over the years [8, 26, 19].

In this paper we adopt the SORA approach [9], since it is flexible and easy to employ together with existing deterministic optimization algorithms. We first define the solution of problem (3.4) as the pair $(\Omega^p, \mathbf{x}^p)$. We note that, $\mathbf{x}^*$ is defined as the Worst Case Scenario obtained for an arbitrary topology, while $\mathbf{x}^p$ is defined as the special Worst Case Scenario obtained with the optimum topology Ω^p.

If, for some reason, $\mathbf{x}^p$ was known beforehand, it would not be necessary to solve problem (3.5) before solving problem (3.4). In this case, the optimum topology Ω^p would be found directly by taking the Worst Case Scenario $\mathbf{x}^p$ in problem (3.4). This puts in evidence that, once the Worst Case Scenario $\mathbf{x}^p$ is known, problem (3.4) becomes a deterministic topology optimization problem. On the other hand, if the optimum topology Ω^p is known, the Worst Case Scenario $\mathbf{x}^p$ can be found directly by solving (3.5) point-wisely with the optimum topology Ω^p.

In practice, neither Ω^p nor $\mathbf{x}^p$ are known beforehand. However, it is possible to start from initial approximations and iterate until accurate solutions are found. In fact, let us indicate some iteration number with (k). Then an iterative algorithm for solving the RBTO problem can be summarized as presented in Algorithm 1. The procedure is started with an arbitrary topology $\Omega^{(0)}$. With this topology we find the Worst Case Scenario $\mathbf{x}^{(0)}$ at each point of interest by solving (3.5) with $\Omega^{(0)}$. From the Worst Case Scenario $\mathbf{x}^{(0)}$ we find a new topology $\Omega^{(1)}$ and so on, until convergence is achieved.

Algorithm 1: Reliability Based Topology Optimization Algorithm

input : Initial topology $\Omega^{(0)}$
output: $(\Omega^p, \mathbf{x}^p)$

Set $k \leftarrow 0$;
Compute $\mathbf{x}^{(0)}$ by solving (3.5) with $\Omega = \Omega^{(0)}$;
while *convergence is not achieved* **do**
  Make $k \leftarrow k + 1$;
  Compute $\Omega^{(k)}$ by solving (3.4) with $\mathbf{x}^* = \mathbf{x}^{(k-1)}$;
  Compute $\mathbf{x}^{(k)}$ by solving (3.5) with $\Omega = \Omega^{(k)}$;
end while
Return $(\Omega^p, \mathbf{x}^p)$ as solution.

We also point out that problem (3.5) can be solved by efficient schemes already developed in the literature. This problem is here solved by using the Advanced Mean Value algorithm, originally proposed in [31]. Besides, in this work the interest points of the structure (the points where we find the Worst Case Scenarios) are taken as Gauss nodes inside the finite elements.

4. Structural Topology Optimization Problem

The RBTO we are dealing with consists in solving problem (3.4) with the Worst Case Scenarios found from problem (3.5). Without loss of generality, we restrict ourselves to uncertainties on the intensity of the applied loads and the stress limit $\overline{\sigma}$ (note that problem stated through (3.5) and (3.4) is general and can be applied when other parameters are random variables). The vector of random variables is then composed by load scale factors of the applied loads and a scale factor

for the stress limit (yielding stress). Considering that $q_1, q_2, ..., q_{m-1}$ are the expected values of the applied loads, we then write the total uncertain applied load q as

$$q = \sum_{i=1}^{m-1} \mathrm{x}_i q_i, \tag{4.1}$$

where $\mathrm{x}_1, \mathrm{x}_2, ..., \mathrm{x}_{m-1}$ are load scale factors. The stress limit, on the other hand, is written as

$$\overline{\sigma} = \mathrm{x}_m \overline{\sigma}_d, \tag{4.2}$$

where x_m represents the stress limit scale factor and $\overline{\sigma}_d$ is the expected value of the stress limit.

In this case, we can use linear superposition of the effects in order to save computational effort. The stress σ and strain ε tensors at each point can be written as

$$\sigma_\Omega := \sum_{i=1}^{m-1} \mathrm{x}_i \sigma(u_i) \quad \text{and} \quad \varepsilon_\Omega := \sum_{i=1}^{m-1} \mathrm{x}_i \varepsilon(u_i). \tag{4.3}$$

The canonical strain $\varepsilon(u_i)$ and stress $\sigma(u_i)$ tensors are obtained from each individual load q_i. For this purpose, we must solve the following set of canonical variational problems related to the structural response when each load q_i is applied: Find $u_i \in \mathcal{V}$ such that

$$\begin{cases} \displaystyle\int_{\mathcal{D}} \sigma(u_i) \cdot \varepsilon(\eta) = \int_{\Gamma_N} q_i \cdot \eta \quad \forall \eta \in \mathcal{V}, \\ \text{with } \sigma(u_i) := \rho \mathbb{C} \varepsilon(u_i), \end{cases} \tag{4.4}$$

$$\tag{4.5}$$

where

$$\varepsilon(\varphi) = \frac{1}{2}(\nabla\varphi + (\nabla\varphi)^\top). \tag{4.6}$$

The space $\mathcal{V}$ is defined as

$$\mathcal{V} := \{\varphi \in H^1(\Omega; \mathbb{R}^2) : \varphi_{|\Gamma_D} = 0\}. \tag{4.7}$$

The piecewise constant function ρ, is defined such as:

$$\rho(x) := \begin{cases} 1, & \text{if } x \in \Omega, \\ \rho_0, & \text{if } x \in \mathcal{D} \setminus \overline{\Omega}, \end{cases} \tag{4.8}$$

with $\rho_0 \ll 1$ used to mimic voids. That is, the structure itself consists of the domain Ω with elastic properties and the remaining part $\mathcal{D} \setminus \overline{\Omega}$, is approximated by means of the two-phase material distribution given by (4.8) over $\mathcal{D}$. The empty region $\mathcal{D} \setminus \overline{\Omega}$ is filled by a material (the soft phase) with Young's modulus, $\rho_0 E$, much lower than the given Young's modulus, E, of the structure material (the hard phase).

Since the topology optimization problem (3.4) is ill-posed, a regularization term given by the strain energy stored in the structure is included [1]. The resulting constrained topology optimization problem is written as follows: Find $\Omega^p \subset \mathcal{D}$, such that

$$\begin{cases} \underset{\Omega \subset \mathcal{D}}{\text{Minimize}}\ \mathcal{J}_\Omega := |\Omega| + \kappa \mathcal{K}_\Omega, \\ \text{subject to: } g_\Omega(\mathbf{x}^*) \leq 0, \end{cases} \tag{4.9}$$

with $\kappa > 0$ and the functional $\mathcal{K}_\Omega$ defined as

$$\mathcal{K}_\Omega = \int_\Omega \sigma_\Omega \cdot \varepsilon_\Omega, \tag{4.10}$$

where σ_Ω and ε_Ω is obtained from (4.3). In addition, the stress constraint in problem (4.9) is imposed by using an efficient class of von Mises stress penalty functional introduced in [6]. Before defining the corresponding penalty functional, let us define the nominal stress S as follows

$$S := \frac{\sigma_\Omega}{\overline{\sigma}}. \tag{4.11}$$

Then, the von Mises stress constraints in terms of normalized stresses are stated as:

$$S_M^2(\mathbf{x}^*) := S_M^2 = \frac{1}{2}\mathbb{B}S \cdot S \leq 1. \tag{4.12}$$

Now, let $\Phi : \mathbb{R}_+ \to \mathbb{R}_+$ be a nondecreasing function of class $\mathcal{C}^2$. We assume that the derivatives Φ' and Φ'' are bounded. Then, the penalty functional is defined as:

$$\mathcal{G}_\Omega := \int_{\Omega^\star} \Phi(S_M^2). \tag{4.13}$$

In particular, we shall adopt a function Φ of the following functional form:

$$\Phi(t) \equiv \Phi_p(t), \tag{4.14}$$

where $p \geq 1$ is a given real parameter and $\Phi_p : \mathbb{R}_+ \to \mathbb{R}_+$ is defined as [3]

$$\Phi_p(t) = [1 + t^p]^{1/p} - 1. \tag{4.15}$$

Therefore, the constrained optimization problem (3.4) with point-wise constraints can be approximated by the following penalized optimization problem:

$$\underset{\Omega \subset \mathcal{D}}{\text{Minimize}}\ \mathcal{J}_\Omega^\alpha := \mathcal{J}_\Omega + \alpha \mathcal{G}_\Omega, \tag{4.16}$$

with the scalar $\alpha > 0$ used to denote a given penalty coefficient. Following the original ideas presented in [6], the local stress constraints in (4.9) are replaced by the penalty functional (4.13). It has been shown in [6] that the unconstrained problem (4.16) is a good approximation to the original constrained problem (4.9) provided that the two following conditions are fulfilled:

- α is large enough in (4.16);
- Φ_p' admits a sharp variation around $t = 1$ in (4.15).

In practice, we chose α as large as possible according to each problem under consideration and p is set as 32, which produces the desired sharp variation of Φ_p' around $t = 1$. See [3] for more details.

In order to simplify further analysis, let us introduce an adjoint state, which is solution of the following boundary value problem:

$$\left\{ \begin{array}{rcll} -\text{div}(\sigma(v)) & = & \text{div}(\chi_{\Omega^\star} k_1(S)\widetilde{\mathbb{B}}S) & \text{in } \mathcal{D}, \\ \sigma(v) & = & \rho\mathbb{C}\varepsilon(v) & \\ v & = & 0 & \text{on } \Gamma_D, \\ \sigma(v)n & = & -\chi_{\Omega^\star} k_1(S)\widetilde{\mathbb{B}}Sn & \text{on } \Gamma_N \cup \Gamma_0, \end{array} \right. \tag{4.17}$$

where the tensor $\widetilde{\mathbb{B}}$ is given by

$$\widetilde{\mathbb{B}} = 6\mu\mathbb{I} + (\lambda - 2\mu)\mathrm{I} \otimes \mathrm{I}. \tag{4.18}$$

The characteristic function $\chi_{\Omega^\star}$ is written as

$$\chi_{\Omega^\star} = \left\{ \begin{array}{ll} 1, & \text{in } \Omega^\star, \\ 0, & \text{otherwise.} \end{array} \right. \tag{4.19}$$

Finally, the function $k_1(S)$ is defined as

$$k_1(S) = \Phi'(S_M^2). \tag{4.20}$$

The deterministic structural optimization problem (4.16) is solved by using the topological derivative concept, which has been shown to be robust with respect to uncertainties on the data [15]. The topological derivative measures the sensitivity of a given shape functional when the topology of the domain is perturbed by insertion of holes, inclusions or source-terms [24]. It is defined through a limit passage when the small parameter governing the size of the topological perturbation goes to zero. Therefore, the topological derivative can be used as a steepest-descent direction in an optimization process like in any method based on the gradient of the cost functional. In contrast to traditional topology optimization methods, the topological derivative formulation does not require a material model concept based on intermediary densities. Thus, interpolation schemes are unnecessary. In addition, it has the advantage of providing an analytic form for the topological sensitivity which allows to obtain the optimal design in few iterations.

In fact, the resulting approach leads to a topology design algorithm of remarkably efficiency and of simple computational implementation, which features only a minimal number of user-defined algorithmic parameters.

For the sake of completeness, the topological derivative associated with the shape functional $\mathcal{J}_\Omega^\alpha$, derived in [6], is stated here in its closed form. Since we are using a very compliant material to mimic voids, the topological derivatives are presented in their limit cases versions when the contrast parameter governing the material properties of the topological perturbations goes to zero or infinity. Finally, the results are written in terms of the Lamé's coefficients, so that they can be used either in plane stress or plane strain assumptions. In particular, the topological derivative of the shape functional $\mathcal{J}_\Omega^\alpha$ is given by the sum

$$D_T\mathcal{J}_\Omega^\alpha(x) = D_T|\Omega|(x) + \kappa D_T\mathcal{K}_\Omega(x) + \alpha D_T\mathcal{G}_\Omega(x), \quad \forall x \in \mathcal{D}. \tag{4.21}$$

We are interested into two particular cases, which are:

Case 1. Let us consider $x \in \Omega$. In this case $\rho = 1$ and the contrast on the material property goes to zero since $\rho_0 \ll 1$. Then the topological derivative $D_T\mathcal{G}_\Omega$ of the von Mises penalty functional reads

$$D_T\mathcal{G}_\Omega = -\mathbb{P}_0 S\cdot\varepsilon(v) - \chi_{\Omega^\star}k_1(S)\mathbb{T}\mathbb{B}S\cdot S + \frac{1}{4}\chi_{\Omega^\star}k_1(S)(10S\cdot S - 2\mathrm{tr}^2 S) + \chi_{\Omega^\star}\Psi(S) - \chi_{\Omega^\star}\Phi(S_M^2), \tag{4.22}$$

where v solves the adjoint problem (4.17). The polarization tensor $\mathbb{P}_0$ is given by [2]

$$\mathbb{P}_0 \;=\; \frac{\lambda+2\mu}{\lambda+\mu}\left(2\mathbb{I} - \frac{\mu-\lambda}{2\mu}\mathrm{I}\otimes\mathrm{I}\right), \tag{4.23}$$

while the fourth order tensor $\mathbb{T}$ is written as

$$\mathbb{T} = a_2\mathbb{I} + \frac{a_1-a_2}{2}\mathrm{I}\otimes\mathrm{I}, \tag{4.24}$$

with

$$a_1 = \frac{\lambda+\mu}{\mu}; \quad a_2 = \frac{\lambda+3\mu}{\lambda+\mu}. \tag{4.25}$$

The function $\Psi(S)$ can be written as

$$\Psi(S) = \frac{1}{\pi}\int_0^1\int_0^\pi \frac{1}{t^2}\left[\Phi(S_M^2+\Lambda(t,\theta)) - \Phi(S_M^2) - \Phi'(S_M^2)\Lambda(t,\theta)\right]d\theta dt, \tag{4.26}$$

where

$$\Lambda(t,\theta) = -\frac{t}{2}\left[5(S_I^2 - S_{I\!I}^2)\cos\theta + 3(S_I - S_{I\!I})^2(2-3t)\cos 2\theta\right] + \frac{t^2}{4}\left[3(S_I+S_{I\!I})^2 + (S_I-S_{I\!I})^2(3(2-3t)^2 + 4\cos^2\theta) + 6(S_I^2 - S_{I\!I}^2)(2-3t)\cos\theta\right], \tag{4.27}$$

with S_I and $S_{I\!I}$ used to denote the eigenvalues of S. Finally, the topological derivative of $\mathcal{K}_\Omega$ is given by

$$D_T\mathcal{K}_\Omega = -\mathbb{P}_0\sigma_\Omega\cdot\varepsilon_\Omega, \tag{4.28}$$

and the topological derivative of the volume reads

$$D_T|\Omega| = -1. \tag{4.29}$$

Case 2. Now, let us consider $x \in \mathcal{D}\setminus\overline{\Omega}$. In this case $x \notin \Omega^\star$ by definition and $\rho = \rho_0 \ll 1$. Therefore, the contrast on the material property goes to infinity. Then the last term in (4.21), namely $D_T\mathcal{G}_\Omega$, is given by

$$D_T\mathcal{G}_\Omega = -\mathbb{P}_\infty S\cdot\varepsilon(v), \tag{4.30}$$

with v solution (4.17). The polarization tensor $\mathbb{P}_\infty$ is written as [2]

$$\mathbb{P}_\infty \;=\; -\frac{\lambda+2\mu}{\lambda+3\mu}\left(2\mathbb{I} + \frac{\mu-\lambda}{2(\lambda+\mu)}\mathrm{I}\otimes\mathrm{I}\right). \tag{4.31}$$

The topological derivative of $\mathcal{K}_\Omega$ is given by

$$D_T\mathcal{K}_\Omega = -\mathbb{P}_\infty\sigma_\Omega \cdot \varepsilon_\Omega, \tag{4.32}$$

and, finally, the topological derivative of the volume assumes

$$D_T|\Omega| = 1. \tag{4.33}$$

The topological derivative with respect to the nucleation of a small circular inclusion with different material property from the background governed by a general contrast can be found in [6].

In fact, the above result (4.21) together with a level-set domain representation method proposed in [4] (see also [7] for more details) is used for solving the deterministic topology optimization problem (3.4) with $\mathbf{x}^* = \mathbf{x}^{(k)}$ fixed, necessary in step (3) of the algorithm proposed in Section 3.3.

5. Numerical Examples

In this section we present some numerical results showing the effectiveness of the proposed methodology. In all numerical examples we assume that the structures are under a plane stress state. The Young's modulus and the Poisson ratio are respectively given by $E = 21000kN/cm^2$ and $\nu = 0.3$ while the strength limit of the material is $\overline{\sigma} = 21kN/cm^2$. Furthermore, $p = 32$ in (4.15) and the contrast on the material property is given by $\rho_0 = 10^{-4}$.

The mechanical problem is discretized into linear triangular finite elements and two steps of uniform mesh refinement were performed during the iterative process. In addition, we consider load intensities and/or stress limit of the material as random variables and linear superposition of effects is used. We also take a target reliability index equal to $\beta_t = 2.0$.

The numerical realizations are driven as follows. We set the hold-all domain as initial guess, namely $\Omega = \mathcal{D}$. The domains $\Omega^\star$ and ω are represented by dark and light grays, respectively. The thick lines represent clamped boundary conditions, while dashed lines means symmetry conditions. If nothing is specified, there is homogeneous Neumann boundary condition.

5.1. **Example 1.** Let us consider a square panel of size $100 \times 100cm^2$ submitted to a distributed loading q, in region of size $50cm$, whose resultant is denoted by $Q = 21kN$, see Fig. 1 for details. The hold-all domain, modeled by using vertical symmetry conditions, is discretized into an initial uniform mesh with 6400 elements and 3281 nodes. The final mesh has 102400 elements and 51521 nodes. Finally, we choose $\kappa = 10$ and $\alpha = 1$.

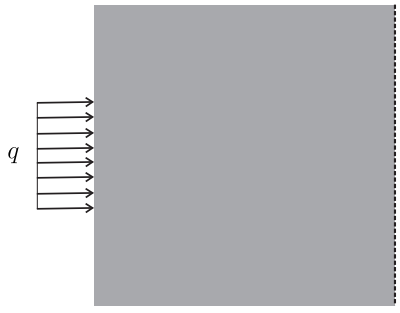

Figure 1. Example 1. Initial guess and boundary conditions.

If topology optimization is made considering all parameters as deterministic, the optimal topology is that presented in Fig. 2(a). In this case, the final result after 27 iterations of the topology optimization algorithm has approximately 51% of volume fraction. Now, we consider the stress limit of the material as a random variable. In particular, we assume that the stress limit scale factor is a Gaussian random variable with unitary mean, namely $\overline{\mathrm{x}} = 1.0$. In the first case, the standard deviation is given by $s = 0.20$. The optimal topology in this case was obtained after 26 iterations of the topology optimization algorithm and it is presented in Fig.

2(b). As expected, the volume of the structure was slightly increased and we have 53% of volume fraction. Next, we repeat the same experiment by setting $s = 0.35$. In this case the final topology, obtained at iteration 32 of the topology optimization algorithm, can be seen in Fig. 2(c). Once again, we observe that the final volume of the structure is increased and we have 57% of volume fraction. Figure 3 shows the obtained stress distributions for all cases at the end of the optimization process. In addition, as can be seen in Table 1, the stress remains under control in all cases.

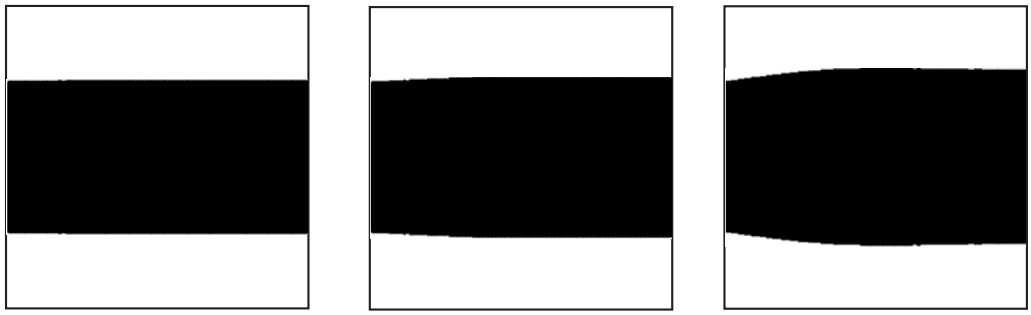

(a) (b) (c)

FIGURE 2. Example 1. Optimal topologies: (a) deterministic optimization $s = 0$, (b) optimization under uncertainties $s = 0.20$, (c) optimization under uncertainties $s = 0.35$.

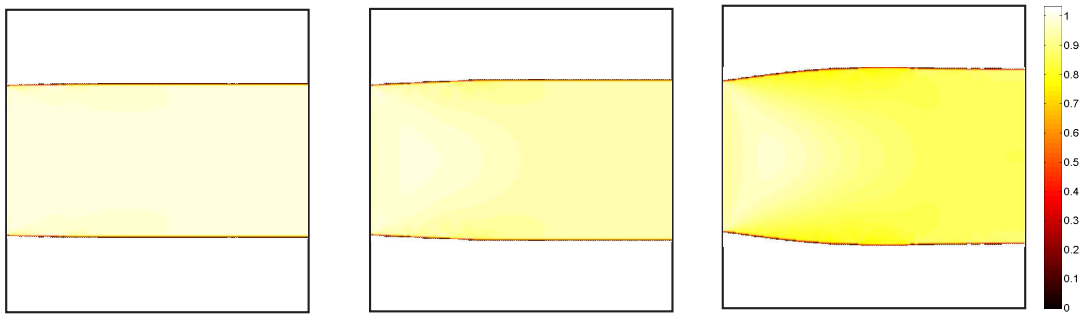

(a) (b) (c)

FIGURE 3. Example 1. Stress distributions: (a) deterministic optimization $s = 0$, (b) optimization under uncertainties $s = 0.20$, (c) optimization under uncertainties $s = 0.35$.

TABLE 1. Example 1. Maximal normalized stress obtained at the end of the iterative process.

	$\max_{\Omega}(S_M)$	vol(%)
$s = 0.00$	1.03	50.75
$s = 0.20$	0.99	52.77
$s = 0.35$	0.97	57.09

5.2. **Example 2.** Let us consider a square panel of size $100 \times 100cm^2$ clamped on its top and submitted to a pair of loads, as shown in Fig. 4. The loading consists of two forces $q_1 = (160.0, -160.0)kN$ and $q_2 = (-160.0, -160.0)kN$ applied on the middle of the bottom edge. No correlation among the random variables is assumed. The stress constraint is not enforced in the light gray region around to the point where the load is applied (see Fig. 4). The hold-all domain is discretized into an initial uniform mesh with 6400 elements and 3281 nodes. The final mesh has 102400 elements and 51521 nodes. In addition, we choose $\kappa = 100$ and $\alpha = 10$.

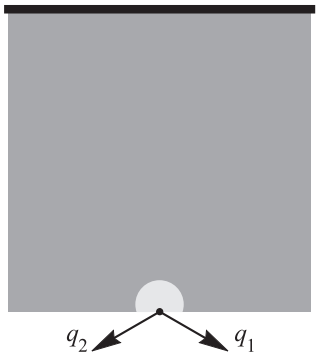

FIGURE 4. Example 2. Initial guess and boundary conditions.

The optimal topology considering all parameters as deterministic was obtained after 25 iterations of the topology optimization algorithm and has 24% of volume fraction. Figure 5(a) shows the solution which is a benchmark to this problem. Next, we consider the load intensities as random variables. In fact, we assume that the load scale factors are represented by Gaussian random variables with unitary mean, namely $\overline{\mathrm{x}}_1 = \overline{\mathrm{x}}_2 = 1.0$. In a first moment we define the standard deviations as $s_1 = s_2 = 0.07$. The optimum topology obtained at iteration 24 of the topology optimization algorithm is presented in Fig. 5(b). The volume of the structure has 34% of volume fraction. As expected, the optimum solution of this case leads to a V-bracket structure, able to handle the horizontal components of the loads that result for cases where the two forces do not have the same intensities. Now, we repeat the same experiment by setting $s_1 = s_2 = 0.15$. In this case the optimal result was obtained after 20 iterations of the topology optimization algorithm with 41% of volume fraction. Figure 5(c) shows the final topology. We observe that the resulting topology also has a V shape with more volume than in the previous case. The stress distributions for all cases at the end of the optimization process are presented in Fig. 6. We note that in all cases under study, the maximum stress does not exceed the threshold within $\Omega^\star$ represented by dark gray color in Fig. 4 .

5.3. **Example 3.** Let us consider the topology design of a tower as shown in Fig. 7. The hold-all domain is given by a T-bracket structure, composed by two rectangles of sizes $200 \times 400cm^2$ and $400 \times 200cm^2$, clamped on the bottom. It is discretized into an initial mesh containing 34412 elements and 17511 nodes. The mesh is intensified at the re-entrant corner in order to capture the stress singularities. The final mesh has 583208 elements and 292845 nodes. The loading consists of a pairs of forces $q_1 = q_2 = (0.0, -120.0)kN$ applied at the two opposites bottom corners of the horizontal branch. The stress constraint is not enforced in the light gray regions of radius $40cm$ centered at the points of load application (see Fig. 7). In addition, we choose $\kappa = 1.5 \times 10^3$ e $\alpha = 10^5$.

In this last example uncertainties are considered during optimization by taking load intensities and stress limit of the material as random variables. No correlation among the random variables is assumed. Therefore, we assume that the load scale factors and stress limit scale factor are represented again by Gaussian random variables with unitary means, namely $\overline{\mathrm{x}}_1 = \overline{\mathrm{x}}_2 = \overline{\mathrm{x}}_3 = 1.0$ and identical standard deviations given by $s_1 = s_2 = s_3 = 0.10$.

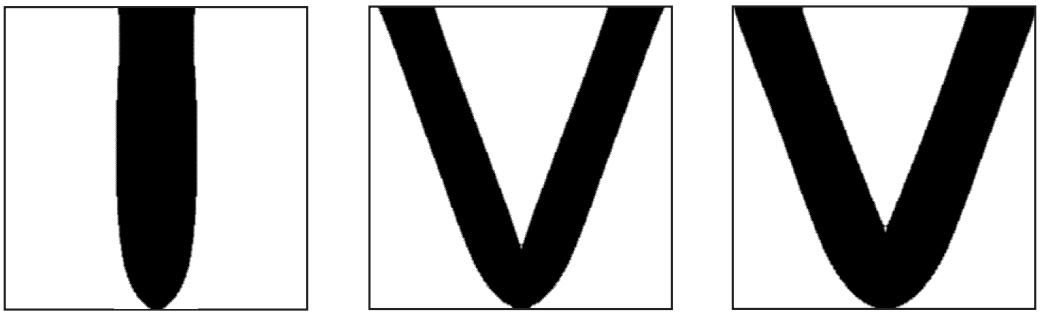

(a) (b) (c)

FIGURE 5. Example 2. Optimal topologies: (a) deterministic optimization $s_1 = s_2 = 0$, (b) optimization under uncertainties $s_1 = s_2 = 0.07$, (c) optimization under uncertainties $s_1 = s_2 = 0.15$.

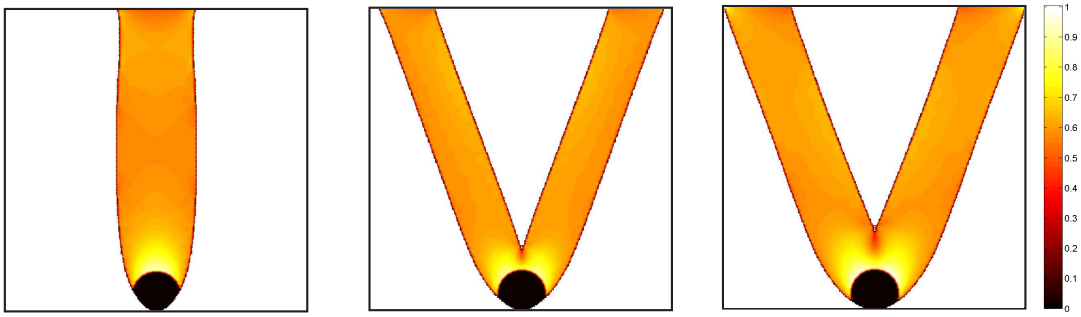

(a) (b) (c)

FIGURE 6. Example 2. Stress distributions: (a) deterministic optimization $s_1 = s_2 = 0$, (b) optimization under uncertainties $s_1 = s_2 = 0.07$, (c) optimization under uncertainties $s_1 = s_2 = 0.15$.

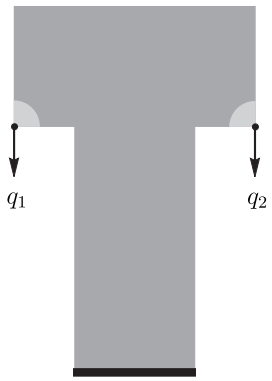

FIGURE 7. Example 3. Initial guess and boundary conditions.

Figure 8(a) presents the optimal topology considering all parameters as deterministic. It was obtained after 82 iterations of the topology optimization algorithm and has 37.5% of volume fraction. Now we consider the uncertainty case. The resulting structure was obtained after 34 iterations of the topology optimization algorithm and it is presented in Fig. 8(b), it has 45.5% of volume fraction.

Figure 9 shows the stress distributions at the end of the optimization process. We observe that in both cases under study, the maximum stress does not exceed the threshold within $\Omega^\star$ represented by dark gray color in Fig. 7. We also highlight that the design obtained considering

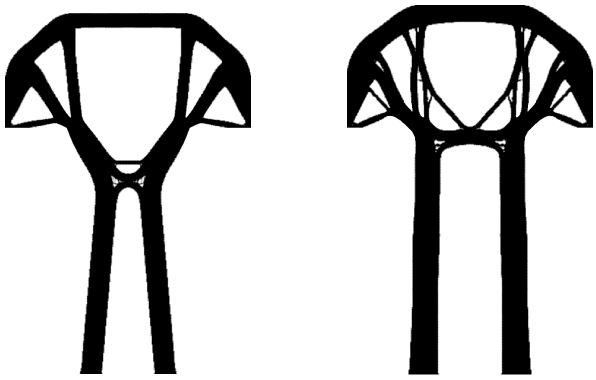

(a) (b)

FIGURE 8. Example 3. Optimal topologies: (a) deterministic optimization $s_1 = s_2 = s_3 = 0$, (b) optimization under uncertainties $s_1 = s_2 = s_3 = 0.10$.

uncertainties is significantly different from the deterministic one. The distributions of the scale factors in the worst case scenario x_1, x_2 and x_3 are shown in Fig. 10. It is interesting to note that the point-wise worst case scenarios present significant variation over the structural domain. The reliability index of the optimum design obtained with Monte Carlo Simulation [21, 23] using 10^5 samples was $\beta = 2.3174$. This reliability index is higher than the target value because the objective function of the topology optimization problem also takes into account the structural compliance, leading to more reliable structures. See discussion in the previous sections.

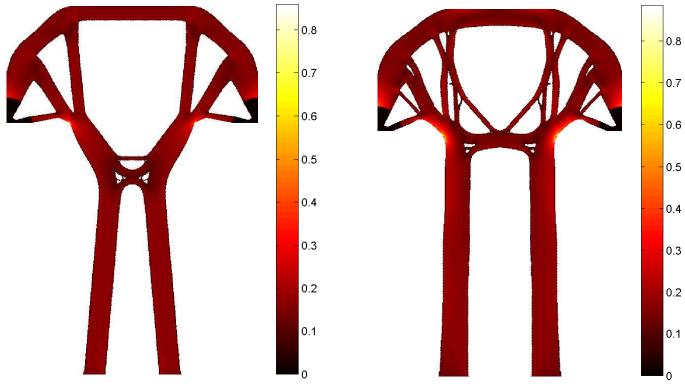

(a) (b)

FIGURE 9. Example 3. Stress distributions: (a) deterministic optimization $s_1 = s_2 = s_3 = 0$, (b) optimization under uncertainties $s_1 = s_2 = s_3 = 0.10$.

6. Conclusion

In this paper an approach for reliability based topology optimization under stress constraints has been presented. Using the Sequential Optimization and Reliability Assessment approach the problem can be rewritten as a deterministic optimization problem with modified parameters, that are obtained with inverse reliability analysis as in the Performance Measure Approach.

This procedure allows us to easily adapt existing deterministic optimization algorithms for the case of reliability based optimization. Here, the deterministic structural topology optimization problem subject to stress constraints has been addressed with an efficient algorithm based on the topological derivative concept and a level-set domain representation method. The examples presented here considered load magnitude and stress limits uncertainties.

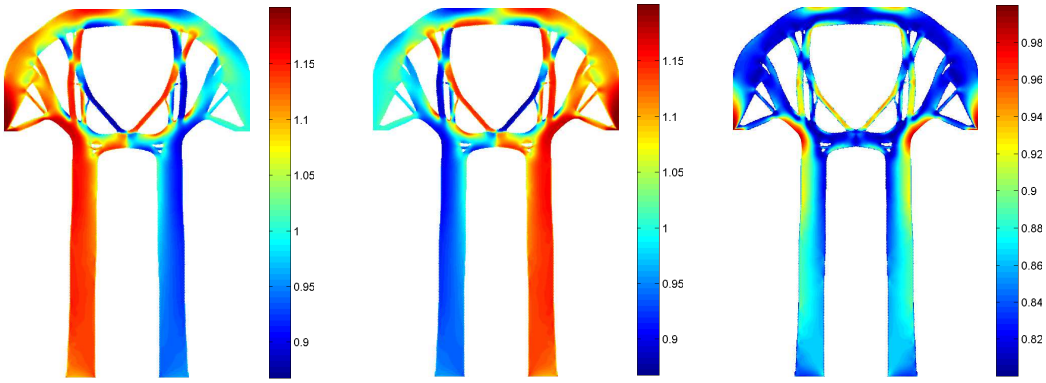

(a) x_1 (b) x_2 (c) x_3

FIGURE 10. Example 3. (a) and (b) load scale factors, (c) stress limit scale factor.

The examples presented show that our approach is able to obtain optimum solutions that take into account data uncertainties. Most important is the fact that the designs obtained considering uncertainties are significantly different – and more acceptable from the physical point of view – than the ones obtained with deterministic optimization only. This indicates that deterministic optimization may not be able to obtain efficient designs in cases subject to significant uncertainties, such as those frequently encountered in practical applications. However, it should be noted that structural topology optimization based on volume minimization under stress constraint is an ill-posed problem. In particular, there is a lack of sufficient optimality conditions for such a topology optimization problem. Therefore, the numerical results presented in this paper are just local minimizers. Finally, we remark that the extension of these ideas to real world problems into three spatial dimensions is not trivial at all and requires further investigation.

ACKNOWLEDGEMENTS

This research was partly supported by CNPq (Brazilian Research Council), CAPES (Brazilian Higher Education Staff Training Agency) and FAPERJ (Research Foundation of the State of Rio de Janeiro). These supports are gratefully acknowledged.

REFERENCES

[1] G. Allaire, F. Jouve, and H. Maillot. Topology optimization for minimum stress design with the homogenization method. *Structural and Multidisciplinary Optimization*, 28(2-3):87–98, 2004.

[2] H. Ammari and H. Kang. *Polarization and moment tensors with applications to inverse problems and effective medium theory*. Applied Mathematical Sciences vol. 162. Springer-Verlag, New York, 2007.

[3] S. Amstutz. A penalty method for topology optimization subject to a pointwise state constraint. *ESAIM: Control, Optimisation and Calculus of Variations*, 16(3):523–544, 2010.

[4] S. Amstutz and H. Andrä. A new algorithm for topology optimization using a level-set method. *Journal of Computational Physics*, 216(2):573–588, 2006.

[5] S. Amstutz and M. A. Ciligot-Travain. A notion of compliance robustness in topology optimization. *ESAIM: Control, Optimisation and Calculus of Variations*, 22(1):64–87, 2016.

[6] S. Amstutz and A. A. Novotny. Topological optimization of structures subject to von Mises stress constraints. *Structural and Multidisciplinary Optimization*, 41(3):407–420, 2010.

[7] S. Amstutz, A. A. Novotny, and E. A. de Souza Neto. Topological derivative-based topology optimization of structures subject to Drucker-Prager stress constraints. *Computer Methods in Applied Mechanics and Engineering*, 233–236:123–136, 2012.

[8] H. Beyer and B. Sendhoff. Robust optimization – a comprehensive survey. *Computer Methods in Applied Mechanics and Engineering*, 196(33–34):3190–3218, 2007.

[9] X. Du and W. Chen. Sequential optimization and reliability assessment method for efficient probabilistic design. *ASME Journal of Mechanical Design*, 126(2):225–233, 2004.

[10] P. Dunning and H. Kim. Robust topology optimization: Minimization of expected and variance of compliance. *American Institute of Aeronautics and Astronautics Journal*, 51(11):2656–2664, 2013.

[11] P. Duysinx and M. P. Bendsøe. Topology optimization of continuum structures with local stress constraints. *International Journal for Numerical Methods in Engineering*, 43:1453–1478, 1998.
[12] H. Emmendoerfer Jr. and E. A. Fancello. A level set approach for topology optimization with local stress constraints. *International Journal for Numerical Methods in Engineering*, 99:129–156, 2014.
[13] Y. Eom, K. Yoo, J. Park, and S. Han. Reliability-based topology optimization using a standard response surface method for three-dimensional structures. *Structural and Multidisciplinary Optimization*, 43(2):287–295, 2011.
[14] A. Haldar and S. Mahadevan. *Reliability assessment using stochastic finite element analysis*. John Wiley & Sons, New York, 2000.
[15] I. Hlaváček, A. A. Novotny, J. Sokołowski, and A. Żochowski. On topological derivatives for elastic solids with uncertain input data. *Journal of Optimization Theory and Applications*, 141(3):569–595, 2009.
[16] G. Kharmanda, N. Olhoff, A. Mohamed, and M. Lemaire. Reliability-based topology optimization. *Structural and Multidisciplinary Optimization*, 26(5):295–307, 2004.
[17] C. Kim, S. Wang, I. Hwang, and J. Lee. Application of reliability-based topology optimization for micro-electromechanical systems. *American Institute of Aeronautics and Astronautics Journal*, 45(12):2926–2934, 2007.
[18] B. S. Lazarov, M. Schevenels, and O. Sigmund. Topology optimization with geometric uncertainties by perturbation techniques. *International Journal For Numerical Methods In Engineering*, 90(11):1321–1336, 2012.
[19] R. H. Lopez and A. T. Beck. Reliability-based design optimization strategies based on FORM: a review. *Journal of the Brazilian Society of Mechanical Sciences and Engineering*, 34(4):506–514, 2012.
[20] Y. Luo, M. Zhou, M. Y. Wang, and Z. Deng. Reliability based topology optimization for continuum structures with local failure constraints. *Computers and Structures*, 143:73–84, 2014.
[21] H. Madsen, S. Krenk, and N. Lind. *Methods of structural safety*. Prentice-Hall, Englewood Cliffs, 1986.
[22] K. Maute and D. M. Frangopol. Reliability-based design of MEMS mechanisms by topology optimization. *Computers and Structures*, 81(8–11):813–824, 2003.
[23] R. Melchers. *Structural reliability analysis and prediction*. John Willey & Sons, Chichester, 1999.
[24] A. A. Novotny and J. Sokołowski. *Topological derivatives in shape optimization*. Interaction of Mechanics and Mathematics. Springer-Verlag, Berlin, Heidelberg, 2013.
[25] J. T. Pereira, E. A. Fancello, and C. S. Barcellos. Topology optimization of continuum structures with material failure constraints. *Structural and Multidisciplinary Optimization*, 26(1–2):50–66, 2004.
[26] G. Schuëller and H. Jensen. Computational methods in optimization considering uncertainties: an overview. *Computer Methods in Applied Mechanics and Engineering*, 198(1):2–13, 2008.
[27] G. A. Silva and E. L. Cardoso. Stress-based topology optimization of continuum structures under uncertainties. *Computer Methods in Applied Mechanics and Engineering*, 313:647–672, 2017.
[28] M. Silva, D. A. Tortorelli, J. A. Norato, C. Ha, and H. Bae. Component and system reliability-based topology optimization using a single-loop method. *Structural and Multidisciplinary Optimization*, 41(1):87–106, 2010.
[29] A. J. Torii, A. A. Novotny, and R. B. Santos. Robust compliance topology optimization based on the topological derivative concept. *International Journal for Numerical Methods in Engineering*, 106(11):889–903, 2016.
[30] J. Tu, K. K. Choi, and Y. H. Park. A new study on reliability-based design optimization. *ASME Journal of Mechanical Design*, 121(4):557–564, 1999.
[31] Y. T. Wu, T. A. Cruse, and H. R. Millwater. Advanced probabilistic structural analysis method for implicit performance functions. *American Institute of Aeronautics and Astronautics Journal*, 28(9):1663–1669, 1990.

(R.B. Santos) Laboratório Nacional de Computação Científica LNCC/MCT, Coordenação de Matemática Aplicada e Computacional, Av. Getúlio Vargas 333, 25651-075 Petrópolis - RJ, Brasil
Email address: renatha@lncc.br

(A.J. Torii) Universidade Federal da Paraíba UFPB, Departamento de Computação Científica, 58051-900, Cidade Universitária, João Pessoa - PB, Brasil
Email address: andre@ci.ufpb.br

(A.A. Novotny) Laboratório Nacional de Computação Científica LNCC/MCT, Coordenação de Matemática Aplicada e Computacional, Av. Getúlio Vargas 333, 25651-075 Petrópolis - RJ, Brasil
Email address: novotny@lncc.br